Chemical Research in Toxicology

Article

pubs.acs.org/crt

Reaction between Peroxynitrite and Triphenylphosphonium-Substituted Arylboronic Acid Isomers: Identification of Diagnostic Marker Products and Biological Implications

Adam Sikora,*[,†,‡] Jacek Zielonka,[†] Jan Adamus,[‡] Dawid Debski,[‡] Agnieszka Dybala-Defratyka,[‡] Bartosz Michalowski,[‡] Joy Joseph,[†] Richard C. Hartley,[§] Michael P. Murphy,[∥] and Balaraman Kalyanaraman*[,†]

[†]Department of Biophysics and Free Radical Research Center, Medical College of Wisconsin, Milwaukee, Wisconsin, United States

[‡]Institute of Applied Radiation Chemistry, Lodz University of Technology, Lodz, Poland

[§]Centre for the Chemical Research of Ageing, WestCHEM School of Chemistry, University of Glasgow, Glasgow G12 8QQ, United Kingdom

[∥]Mitochondrial Biology Unit, Medical Research Council, Cambridge, United Kingdom

Supporting Information

ABSTRACT: Aromatic boronic acids react rapidly with peroxynitrite ($ONOO^-$) to yield phenols as major products. This reaction was used to monitor $ONOO^-$ formation in cellular systems. Previously, we proposed that the reaction between $ONOO^-$ and arylboronates ($PhB(OH)_2$) yields a phenolic product (major pathway) and a radical pair $PhB(OH)_2O^{\bullet-}\cdots{}^{\bullet}NO_2$ (minor pathway). [Sikora, A. et al. (2011) *Chem. Res. Toxicol. 24*, 687−697]. In this study, we investigated the influence of a bulky triphenylphosphonium (TPP) group on the reaction between $ONOO^-$ and mitochondria-targeted arylboronate isomers (*o*-, *m*-, and *p*-$MitoPhB(OH)_2$). Results from the electron paramagnetic resonance (EPR) spin-trapping experiments unequivocally showed the presence of a phenyl radical intermediate from *meta* and *para* isomers, and not from the *ortho* isomer. The yield of *o*-$MitoPhNO_2$ formed from the reaction between *o*-$MitoPhB(OH)_2$ and $ONOO^-$ was not diminished by phenyl radical scavengers, suggesting a rapid fragmentation of the *o*-$MitoPhB(OH)_2O^{\bullet-}$ radical anion with subsequent reaction of the resulting phenyl radical with ${}^{\bullet}NO_2$ in the solvent cage. The DFT quantum mechanical calculations showed that the energy barrier for the dissociation of the *o*-$MitoPhB(OH)_2O^{\bullet-}$ radical anion is significantly lower than that of *m*-$MitoPhB(OH)_2O^{\bullet-}$ and *p*-$MitoPhB(OH)_2O^{\bullet-}$ radical anions. The nitrated product, *o*-$MitoPhNO_2$, is not formed by the nitrogen dioxide radical generated by myeloperoxidase in the presence of the nitrite anion and hydrogen peroxide, indicating that this specific nitrated product may be used as a diagnostic marker product for $ONOO^-$. Incubation of *o*-$MitoPhB(OH)_2$ with RAW 264.7 macrophages activated to produce $ONOO^-$ yielded the corresponding phenol *o*-MitoPhOH as well as the diagnostic nitrated product, *o*-$MitoPhNO_2$. We conclude that the *ortho* isomer probe reported here is most suitable for specific detection of $ONOO^-$ in biological systems.

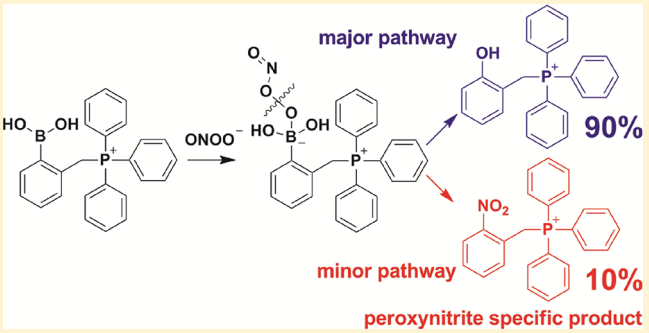

INTRODUCTION

Recent research has focused on the development of targeted probes for detecting mitochondrial reactive oxygen and nitrogen species (ROS/RNS).[1,2] One of the ways in which a small molecule probe can be transported to mitochondria is through covalent attachment to a lipophilic, delocalized positively charged triphenylphosphonium (TPP) cation.[3] Because of both the cationic and lipophilic character, chemical probes tagged with TPP cation accumulate preferentially within mitochondria.

Arylboronic acids react with hydrogen peroxide stoichiometrically to form the corresponding phenols.[4] Recently, boronate-based fluorogenic probes were synthesized for detecting cellular hydrogen peroxide.[5,6] Mitochondria-targeted TPP chemical probes were designed to detect mitochondrial ROS (MitoPY, MitoTEMPO-H).[7,8] Arylboronic-based TPP probe MitoB [*m*-$MitoPhB(OH)_2$, (2-boronobenzyl)-triphenylphosphonium salt] (Figure 1) was used to detect H_2O_2 in living *Drosophila*.[9,10] In this study, we investigated the reaction between peroxynitrite ($ONOO^-$) and the three isomers of MitoB.

Our previous studies have shown that arylboronates can be oxidized not only by H_2O_2 but also by other biologically

Received: December 12, 2012

   dx.doi.org/10.1021/tx300499c | *Chem. Res. Toxicol.* XXXX, XXX, XXX−XXX

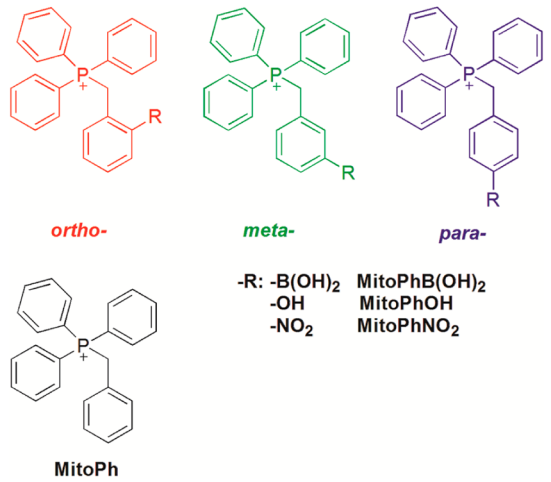

Figure 1. Structures of MitoPhB$(OH)_2$ isomers and the major and minor products of their reactions with peroxynitrite.

relevant oxidants including hypochlorite and $ONOO^-$.[11,12] Results showed that boronate-based fluorogenic probes are suitable for real time monitoring of $ONOO^-$ formed in cell-free systems and in activated macrophages.[13,14] Peroxynitrite[15,16] reacts with arylboronates rapidly ($k \sim 10^6$ $M^{-1}s^{-1}$ at pH 7.4) and stoichiometrically. The major oxidation products are phenols (yield ~85–90%).[11] The minor products (10–15%) are formed via a radical pathway of the reaction.[12] The proposed mechanism for the reaction between $ONOO^-$ and arylboronates is presented in Scheme 1. The initial step of the reaction involves the formation of an anionic adduct between $ONOO^-$ and the boronate. Further cleavage of the O–O bond results in the formation of phenol and nitrite (major, heterolytic O–O cleavage pathway) or caged radical pair PhB-$(OH)_2O^{\bullet-}\cdots{}^{\bullet}NO_2$ (minor, homolytic O–O cleavage pathway). The subsequent fragmentation of the $PhB(OH)_2O^{\bullet-}$ radical anion leads to the formation of phenyl radical $Ph^{\bullet}$ that reacts with H-atom donors, nitrogen dioxide $^{\bullet}NO_2$, or molecular oxygen.

Here, we compared the reaction profiles of $ONOO^-$ with three isomeric TPP^+-substituted phenylboronic acids (*o*-MitoPhB$(OH)_2$, *m*-MitoPhB$(OH)_2$, and *p*-MitoPhB$(OH)_2$) (Figure 1). We determined that the yield of *o*-MitoPhNO_2 formed from the reaction of *o*-MitoPhB$(OH)_2$ with $ONOO^-$ is unaffected by the phenyl radical scavengers, suggesting fast fragmentation of the *o*-MitoPhB$(OH)_2O^{\bullet-}$ radical anion with subsequent reaction of the resulting phenyl radical with $^{\bullet}NO_2$ in the solvent cage. Moreover, even in the presence of 2-propanol, *o*-MitoPhNO_2 is formed in relatively high yield (9%). This is 9 times higher than that of *m*-MitoPhNO_2 and *p*-MitoPhNO_2 under the same conditions. We conclude that determination of both major and minor products from *o*-MitoPhB$(OH)_2$ will serve as a unique tool providing a diagnostic marker for cellular $ONOO^-$ formation.

EXPERIMENTAL PROCEDURES

Chemicals. MitoPhB$(OH)_2$ isomers, MitoPhNO_2, and MitoPh were synthesized according to a published procedure of triphenylphosphine benzylation.[17] All solutions were prepared using deionized water (Millipore Milli-Q system). $ONOO^-$ was prepared according to the published procedure,[18] by reacting nitrite with H_2O_2. The concentration of $ONOO^-$ was determined by measuring the absorbance at 302 nm ($\varepsilon = 1.7 \times 10^3$ $M^{-1}cm^{-1}$) in alkaline aqueous solutions (pH > 12).[18] DPTA-NONOate[19,20] was from Cayman Chemicals. Xanthine oxidase (XO) and myeloperoxidase (MPO) were obtained from Sigma, and catalase was from Boehringer. All other reagents (of the highest purity available) were from Sigma-Aldrich Corp.

Determination of $O_2^{\bullet-}$ and $^{\bullet}NO$ Fluxes. $^{\bullet}NO$ and $O_2^{\bullet-}$ fluxes were determined in phosphate buffer (100 mM, pH 7.4) containing dtpa (100 μM) as described previously.[14] Briefly, $^{\bullet}NO$ fluxes were determined by measuring the rate of the decomposition of DPTA-NONOate by following the decrease in absorbance at 250 nm ($\varepsilon = 8 \times 10^3$ M^{-1} cm^{-1}).[19] Assuming that two molecules of $^{\bullet}NO$ are released from the nitric oxide donor, the measured rate of NONOate decomposition was multiplied by a factor of 2 to obtain the rate of $^{\bullet}NO$ release. The superoxide was generated from XO catalyzed oxidation of hypoxanthine (HX). The flux of $O_2^{\bullet-}$ was determined by monitoring the superoxide dismutase-inhibitable reduction of cytochrome *c* following the increase in absorbance at 550 nm ($\Delta\varepsilon = 2.1 \times 10^4$ $M^{-1}cm^{-1}$).[21]

HPLC and UPLC/MS Analyses. HPLC analyses were performed using an Agilent 1100 HPLC system equipped with fluorescence and UV–vis absorption detectors. In the studies on the reaction profile of peroxynitrite oxidation of MitoPhB$(OH)_2$ isomers, 100 μL of sample was injected into the HPLC system equipped with a C_{18} column (Phenomenex, Kinetex, 100 × 4.6 mm, 2.6 μm) equilibrated with 10% CH_3CN [containing 0.1% (v/v) trifluoroacetic acid (TFA)] in 0.1% TFA aqueous solution. The compounds were separated by a linear

Scheme 1

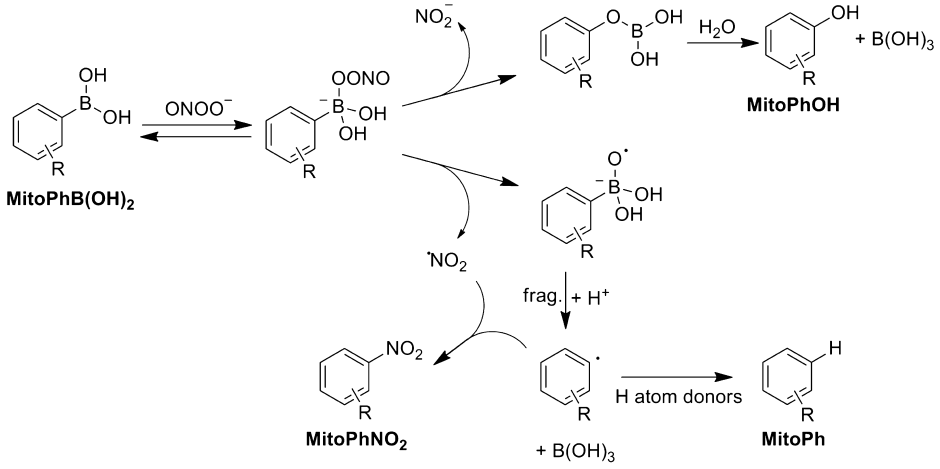

dx.doi.org/10.1021/tx300499c | Chem. Res. Toxicol. XXXX, XXX, XXX–XXX

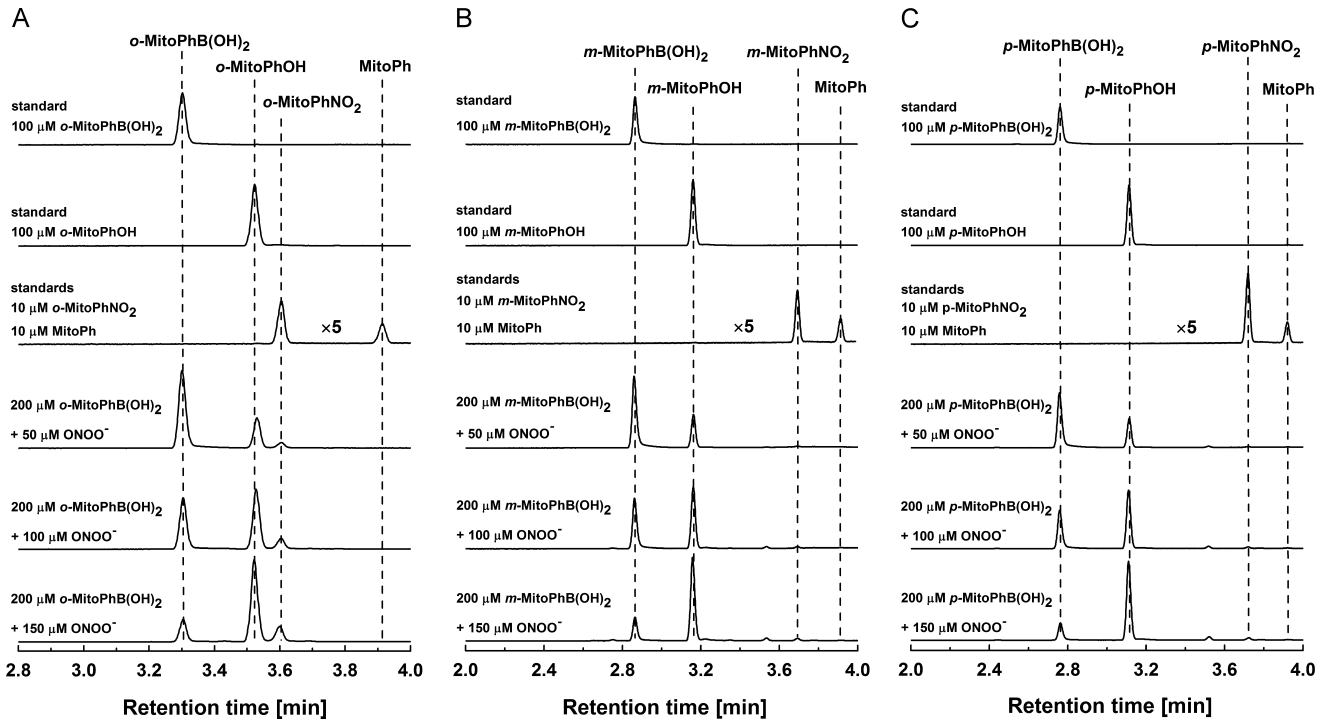

Figure 2. UPLC analyses of products formed from the reaction between triphenylphosphonium-substituted arylboronic acids and peroxynitrite. (A) *o*-MitoPhB$(OH)_2$, (B) *m*-MitoPhB$(OH)_2$, and (C) *p*-MitoPhB$(OH)_2$. Incubation mixtures consisting of 200 μM *o*-, *m*-, and *p*-MitoPhB$(OH)_2$ in phosphate buffer (pH 7.4, 50 mM) containing dtpa (100 μM) and peroxynitrite at the indicated concentration. *o*-, *m*-, and *p*-MitoPhB$(OH)_2$ and their corresponding oxidation products were detected using UV absorption detection at 268 ± 1.2 nm.

increase in CH_3CN phase concentration from 10 to 100% over 7 min, using a flow rate of 1.5 mL/min. Under these conditions, the following retention times (in min) were observed: *o*-MitoPhB$(OH)_2$, 4.31; *o*-MitoPhOH, 4.50; *o*-MitoPhNO$_2$, 4.61; MitoPh, 4.82; *m*-MitoPhB$(OH)_2$, 4.05; *m*-MitoPhOH, 4.2; *m*-MitoPhNO$_2$, 4.70; *p*-MitoPhB$(OH)_2$, 3.98; *p*-MitoPhOH, 4.24; and *p*-MitoPhNO$_2$, 4.71. The peak areas detected by monitoring the absorption at 268 nm were used for the quantitation.

To characterize the synthesized triphenylphosphonium compounds and to identify the products of the reaction of peroxynitrite with triphenylphosphonium-substituted arylboronic acids, the UPLC/MS analyses were performed using an Acquity UPLC Waters Ltd. system coupled online to an LCT Premier XE (Waters) mass spectrometer with a ToF mass detector. One microliter of sample was injected into the UPLC system equipped with a C_{18} column (Waters Acquity BEH C18, 100 × 2.1 mm, 1.7 μm) maintained at 40 °C and equilibrated with 30% CH_3CN [containing 0.1% (v/v) trifluoroacetic acid (TFA)] in 0.1% TFA aqueous solution. The compounds were separated by a linear increase in CH_3CN phase concentration from 30 to 60% from 0.8 to 4 min, using a flow rate of 0.35 mL/min. Under these conditions, the following retention times (in min) were observed: *o*-MitoPhB$(OH)_2$, 3.30; *o*-MitoPhOH, 3.52; *o*-MitoPhNO$_2$, 3.59; MitoPh, 3.91; *m*-MitoPhB$(OH)_2$, 2.86; *m*-MitoPhOH, 3.16; *m*-MitoPhNO$_2$, 3.69; *p*-MitoPhB$(OH)_2$, 2.76; *p*-MitoPhOH, 3.11; and *p*-MitoPhNO$_2$, 3.72. The compounds were detected by monitoring the absorption at 268 ± 1.2 nm. The mass spectrometer was operated in W mode with lock mass correction. Lock mass solution (leucine-enkephalin, reference mass: $[M + H]^+$ 556.2771; $[M + H]^+$ 557.2801) was prepared at a concentration of 0.5 ng/μL in 50:50 (v/v), water/acetonitrile solution and stored in 4 °C until further use. Data acquisition and analyses were performed using the MassLynx 4.1 data system software (Waters) and OriginPro 8.6 (OriginLab).

To investigate the effect of MitoPhB$(OH)_2$ isomers on the oxidation and nitration of tyrosine, 100 μL of sample was injected into the HPLC system equipped with a Phenomenex Synergi 4u Hydro-RP 80 Å column (250 × 4.6 mm, 4 μm) equilibrated with water containing 0.1% (v/v) TFA. The compounds were separated by a linear increase in CH_3CN phase (containing 0.1% (v/v) TFA) concentration from 0 to 5% over 20 min, then further linear increase in CH_3CN phase concentration from 5 to 100% over the next 30 min, using a flow rate of 1.0 mL/min. Under those conditions, tyrosine eluted at 19.7 min, nitrotyrosine at 27.9 min, and dityrosine at 25.8 min. Formation of dityrosine was monitored with the use of a fluorescence detector ($\lambda_{ex.}$ = 284 nm; $\lambda_{em.}$ = 410 nm), and nitrotyrosine was monitored at 350 nm with the use of absorption detector.

UV−Vis Absorption Measurements. The UV−vis absorption spectra were collected using an Agilent 8453 spectrophotometer equipped with a photodiode array detector and thermostatted cell holder.

EPR Experiments. All electron paramagnetic resonance (EPR) spectra were collected using a Bruker EMX spectrometer.

ABTS Oxidation. Typically, incubation mixtures used in EPR experiments on ABTS oxidation consisted of 500 μM ABTS and 250 μM MitoPhB$(OH)_2$ isomer in phosphate buffer (100 mM, pH 7.4) containing dtpa (100 μM) and were rapidly mixed with bolus $ONOO^-$ (250 μM). Samples were subsequently transferred to a 100 μL capillary tube, and EPR measurements were started within 30 s after the bolus addition of peroxynitrite. Spectrometer parameters were as follows: scan range, 60 G; field set, 3505 G; time constant, 1.28 ms; scan time, 42 s; modulation amplitude, 0.2 G; modulation frequency, 100 kHz; receiver gain, 2 × 10^5; and microwave power, 20 mW. The spectra shown are the averages of 10 scans.

EPR Spin-Trapping Experiments. Typically, incubation mixtures used in spin-trapping experiments consisted of 250 μM MitoPhB$(OH)_2$ isomer and MNP spin trap (40 mM) in phosphate buffer (100 mM, pH 7.4) containing dtpa (100 μM) and 5% CH_3CN. Solutions were rapidly mixed with bolus $ONOO^-$ (200 μM). Samples were subsequently transferred to an EPR capillary tube, and spectra were recorded. Spectrometer parameters were as follows: scan range, 75 G; modulation amplitude, 1.0 G; and receiver gain, 1 × 10^5. The spectra shown are the averages of 10 scans.

Theoretical Studies. All calculations were performed with the use of the Gaussian 09, rev.A.02 (G09), package.[22] The electronic structure calculations were carried out using the M06−2X function

dx.doi.org/10.1021/tx300499c | Chem. Res. Toxicol. XXXX, XXX, XXX−XXX

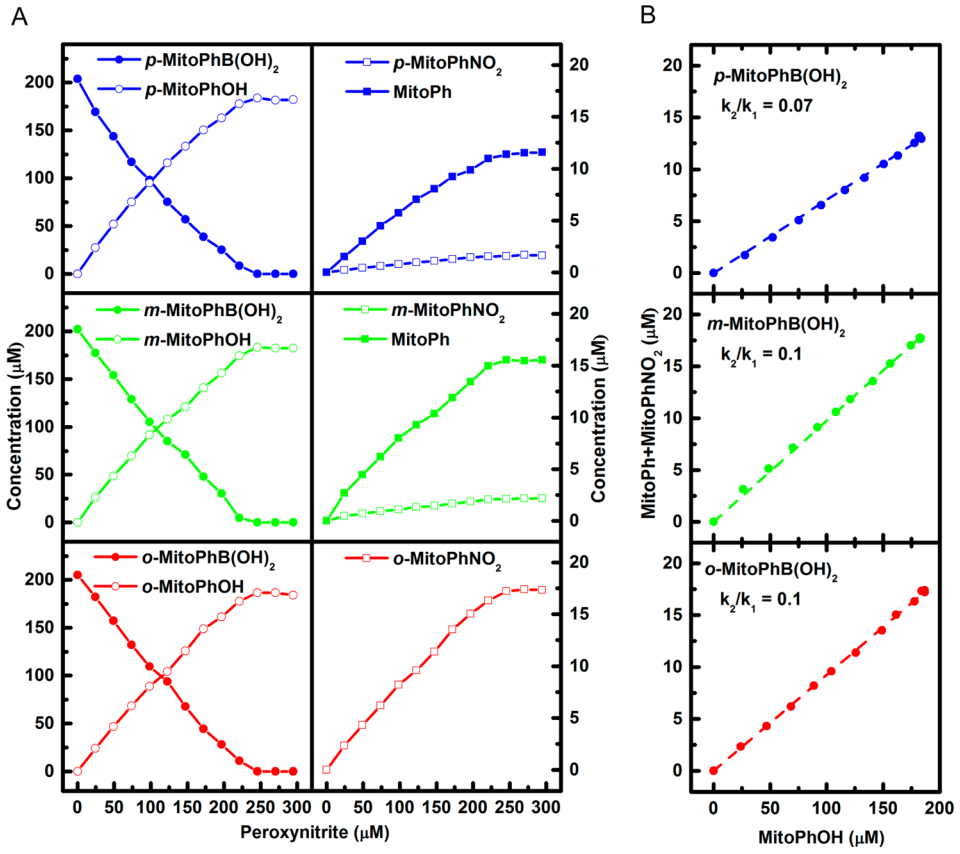

Figure 3. Relationship between substrate depletion and major/minor product formation during the peroxynitrite reaction with $MitoPhB(OH)_2$. (A) Incubation mixtures consisted of 200 μM $MitoPhB(OH)_2$ in phosphate buffer (pH 7.4, 100 mM) containing dtpa (100 μM), 10% 2-PrOH, and catalase (100 U/mL). After bolus addition of peroxynitrite, the reaction mixtures were analyzed using the HPLC/UV method. $MitoPhB(OH)_2$ and the products were detected at 268 nm. Each point represents the average value of three samples. The concentrations were determined based on the calibration curves obtained for authentic standards. MitoPhOH standards were prepared by oxidation of $MitoPhB(OH)_2$ in the presence of excess of H_2O_2 (incubation mixture contained $MitoPhB(OH)_2$ in phosphate buffer (pH 7.4, 100 mM) and dtpa (100 μM), 10% 2-PrOH, and 10 mM H_2O_2). The standard deviations are smaller than the point's size. (B) Analysis of the ratio of minor products (sum of MitoPh + $MitoPhNO_2$) and the major product (MitoPhOH). The ratio of the rate constants of homolytic (k_2) and heterolytic (k_1) cleavage pathways was estimated.

of Truhlar and co-workers[23,24] with the 6-31+G(d,p) basis set.[25,26] Initial geometry of the three isomeric $MitoPhB(OH)_2O^{\bullet-}$ radical anions was fully optimized and used for the relaxed potential energy scan performed along the reaction coordinate defined as an elongating boron−carbon bond length. All structures on the potential energy surfaces were fully optimized, and the stationary points were confirmed by performing harmonic vibrational analysis. Local minima were characterized by 3N-6 real normal modes of vibrations, whereas the transition states had exactly one imaginary frequency. The influence of the environment was modeled using the polarizable continuum solvent model (PCM)[27] with parameters for water as implemented in G09. Open shell species were treated using the unrestricted Hartree−Fock (UHF) method.[28] We have used the default convergence and optimization criteria in all calculations performed using the Gaussian package.

Cell Culture. RAW 264.7 macrophages were cultured in DMEM medium supplemented with 10% FBS. Details on the culturing conditions and protocol for stimulation of macrophages to produce $ONOO^-$ have been published elsewhere.[14] For stimulation of $^{\bullet}NO$ production, the cells were incubated overnight (12−16 h) with LPS (1 μg/mL) and IFNγ (50 U/mL). For stimulation of $O_2^{\bullet-}$ production, cells were treated with 1 μM PMA. Co-stimulation of $^{\bullet}NO$ and $O_2^{\bullet-}$ production leads to the generation of $ONOO^-$, as shown previously.[13,14]

RESULTS

Reaction of $MitoPhB(OH)_2$ with $ONOO^-$. The second-order rate constants for the reaction between peroxynitrite and mitochondria-targeted arylboronates for *ortho*, *meta*, and *para* isomers were determined to be $(3.5 \pm 0.5) \times 10^5$, $(1 \pm 0.1) \times 10^6$, and $(1 \pm 0.1) \times 10^6$ $M^{-1}s^{-1}$, respectively. The rate constants were determined by competition kinetics with resorufin boronate as a standard ($k = (1 \pm 0.1) \times 10^6$ $M^{-1}s^{-1}$) using pulse radiolysis; the identity of the oxidizing species was confirmed by the inhibitory effect of superoxide dismutase on the yield of resorufin (unpublished data). Both *para* and *meta* isomers react with $ONOO^-$ with the rate constant close to the value of 1×10^6 $M^{-1}s^{-1}$, previously determined for phenylboronic acids.[11,13] However, the rate constant of the reaction of peroxynitrite with the *ortho* isomer is 3-fold lower, possibly due to the steric hindrance of the bulky triphenylphosphonium moiety. Nonetheless, the rate constants of the reaction of peroxynitrite with all three isomers of $MitoPhB(OH)_2$ are several orders of magnitude higher than that reported for the reaction of *m*-$MitoPhB(OH)_2$ with hydrogen peroxide ($k = 3.8$ $M^{-1}s^{-1}$ at pH 8; $T = 25$ °C).[9]

Identification and Quantitation of Products Formed from Oxidation of $MitoPhB(OH)_2$ Isomers. The structures of the oxidation products of $MitoPhB(OH)_2$ were determined by mass spectral analysis and by comparison with synthesized

dx.doi.org/10.1021/tx300499c | Chem. Res. Toxicol. XXXX, XXX, XXX−XXX

authentic standards (Figure 2). Table S1 (see Supporting Information) lists the mass spectral parameters for the isomers of MitoPhB$(OH)_2$ and their major and minor oxidation products. As shown in Figure 2A, oxidation of *o*-MitoPhB$(OH)_2$ by peroxynitrite in phosphate buffer (pH 7.4) leads to the formation of two oxidation products: *o*-MitoPhOH (the major product) and *o*-MitoPhNO_2, whereas the oxidation of two other MitoPhB$(OH)_2$ isomers results mainly in the formation of corresponding phenols, with much lower yields of the nitrated products (Figures 2B and C). The reaction between aryl boronic acids and $ONOO^-$ is stoichiometric, as the yield of boronate consumption is close to 100% with respect to the amount of peroxynitrite (Figure 3A).

To characterize the reactions in more detail, the profiles of formation of the major and minor products (MitoPhOH, MitoPhNO_2, and MitoPh, Figure 1) formed during the reaction between $ONOO^-$ and MitoPhB$(OH)_2$ isomers were investigated. We used the HPLC technique to determine the amount of major and minor products formed during the reaction with peroxynitrite in the presence of 2-PrOH, an efficient phenyl radical scavenger. The consumption of substrates and the amount of products formed in the reaction with peroxynitrite were determined based on the calibration curves obtained for the boronate isomers MitoPhB$(OH)_2$ and the oxidation products MitoPhOH, MitoPhNO_2 isomers, and MitoPh.

Figure 3A shows substrate depletion and product formation during the reaction between MitoPhB$(OH)_2$ isomers and $ONOO^-$. Boronates (250 μM) in phosphate buffer (100 mM, pH 7.4) containing dtpa (100 μM), 10% 2-PrOH, and catalase (100 U/mL) were rapidly mixed with $ONOO^-$ (10−300 μM). Previously, we have shown that the addition of phenyl radical scavengers (e.g., 2-PrOH) to the reaction mixtures is a convenient way to estimate the yield of minor products formed during the reaction between arylboronates and peroxynitrite.[12] In the presence of 2-propanol, the phenyl radical formed in the radical pathway is almost quantitatively converted into the product in which the boronate moiety is replaced by a hydrogen atom, with a smaller fraction undergoing a recombination reaction with $^{\bullet}NO_2$. We have shown that the sum of MitoPh and MitoPhNO_2 formed reflects the total amount of phenyl radicals produced. The enzyme, catalase, was used to inhibit the oxidation of boronates by H_2O_2 that can be formed after the hydrogen atom abstraction from 2-PrOH by phenyl radicals in the presence of oxygen.

As shown in Figure 3A, the extent of boronate consumption in the presence of $ONOO^-$ and the formation of major phenolic product, MitoPhOH, are very similar for all isomers. However, the relative yields of the minor product of the reaction between $ONOO^-$ and MitoPhB$(OH)_2$ are different. With *para* and *meta* isomers, the dominant minor product formed from the radical pathway in the presence of 10% 2-PrOH (an effecient phenyl radical scavenger) is MitoPh, whereas with the *ortho* isomer, the only minor product detected was *o*-MitoPhNO_2. More importantly, *o*-MitoPhNO_2 formation was not observed in the MPO/H_2O_2/NO_2^- system generating $^{\bullet}NO_2$ (Figure 4). In this system, *o*-MitoPhOH formed in the reaction between *o*-MitoPhB$(OH)_2$ and H_2O_2 is efficiently nitrated by $^{\bullet}NO_2$ produced by the MPO/H_2O_2/NO_2^- system, as evidenced by the formation of two isomeric nitration products of *o*-MitoPhOH (e.g., $C_{25}H_{21}NO_3P$) (see Figure 4 and Table S2 in Supporting Information).

Assuming that MitoPhOH, the major product of MitoPhB$(OH)_2$ oxidation by peroxynitrite, is produced exclusively via

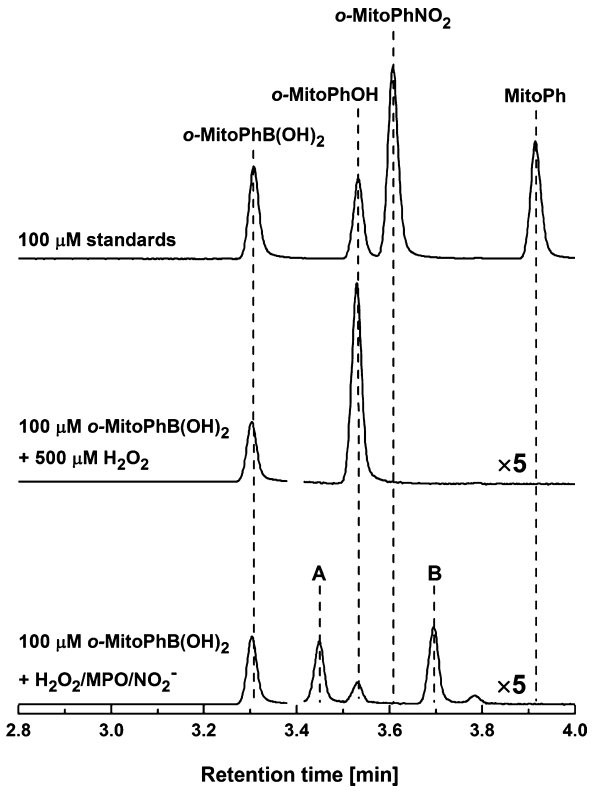

Figure 4. UPLC analyses of products formed from *o*-MitoPhB$(OH)_2$ in the MPO/H_2O_2/nitrite system. Incubation mixtures contained *o*-MitoPhB$(OH)_2$ (100 μM), H_2O_2 (500 μM), MPO (5 U/mL), and $NaNO_2$ (500 μM) in phosphate buffer (pH 7.4, 50 mM) with dtpa (100 μM). The reaction was initiated by the addition of H_2O_2. Products were determined 40 min after adding H_2O_2 at 268 ± 1.2 nm. A and B indicate two isomeric nitration products of *o*-MitoPhOH (general formula, $C_{25}H_{21}NO_3P$) as determined with the use of an MS detector (see Table S2 in Supporting Information).

the nonradical pathway and is not consumed under the experimental conditions, and that all the minor products (MitoPh and MitoPhNO_2) are formed through the radical pathway (from the fragmentation of MitoPhB$(OH)_2O^{\bullet-}$), the ratios of the rate constants of the radical (homolytic cleavage of the O−O bond) and nonradical (heterolytic cleavage of the O−O bond) pathways were determined from the plot of the sum of the minor products versus the amount of MitoPhOH formed (Figure 3B).

The selective formation of *o*-MitoPhNO_2 as the predominant minor product from the $ONOO^-$/*o*-MitoPhB$(OH)_2$ reaction is unique and significant from a diagnostic perspective involving the detection of $ONOO^-$. Therefore, we also investigated the influence of some biologically relevant reductants, glutathione, NADH, and ascorbate, on minor oxidation products' profiles and found an effect similar to that seen with 2-PrOH. Glutathione and ascorbate are known to react with peroxynitrite (the reported rate constants are $k = 1.3 \times 10^3$ $M^{-1}s^{-1}$ for glutathione, at 37 °C and pH 7.5,[29] and $k = 1 \times 10^6$ $M^{-1}s^{-1}$ for the formation of an adduct of ONOOH to monohydrogen ascorbate at pH 5.8[30]). Therefore, although GSH decreased the consumption of *o*-MitoPhB$(OH)_2$ by *ca.* 15% (Figure 5A), this cannot be explained by simple competition with boronate for $ONOO^-$. Of note, the reported rate constant of the reaction of ONOOH with monohydroascorbate[30] seems to be overestimated, as one would expect

dx.doi.org/10.1021/tx300499c | *Chem. Res. Toxicol.* XXXX, XXX, XXX−XXX

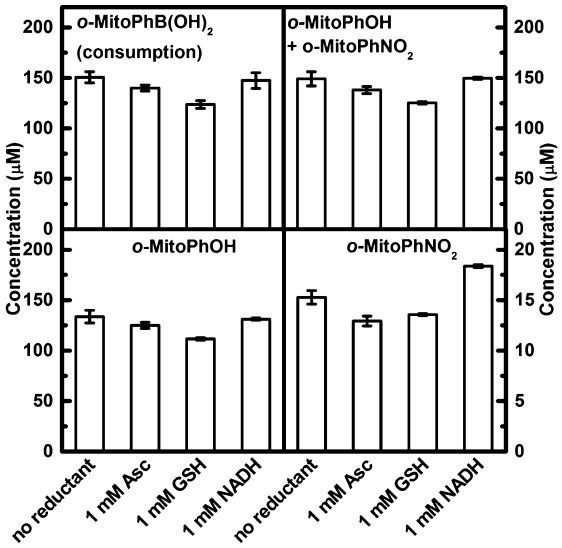

Figure 5. Effects of ascorbate, glutathione, and NADH on substrate depletion and major/minor product formation. Incubation mixtures consisted of 250 μM *o*-MitoPhB(OH)$_2$ in phosphate buffer (pH 7.4, 100 mM) containing dtpa (100 μM), catalase (100 U/mL), and the reductant (as indicated). After a bolus addition of peroxynitrite (resulting in the 150 μM peroxynitrite concentration in the sample), the reaction mixtures were analyzed by HPLC/UV. Each bar represents the average value of three samples. The error bars represent standard deviations.

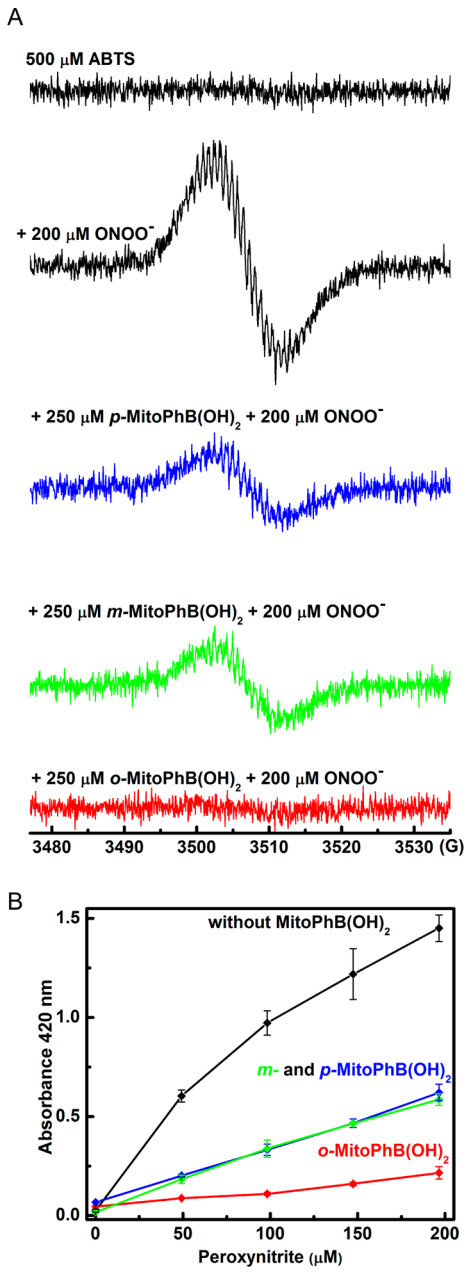

Figure 6. Oxidation of ABTS by oxidants formed from the MitoPhB(OH)$_2$ reaction with peroxynitrite. (A) Incubation mixtures consisted of 500 μM ABTS and 250 μM MitoPhB(OH)$_2$ (if indicated) in phosphate buffer (pH 7.4, 100 mM) containing dtpa (100 μM). The reaction mixture was transferred to an EPR capillary immediately after bolus addition of ONOO$^-$ (resulting in the 200 μM peroxynitrite concentration in the sample), and the spectra were recorded at room temperature. (B) Incubation mixtures consisted of 500 μM ABTS and 250 μM MitoPhB(OH)$_2$ (as indicated) in phosphate buffer (pH 7.4, 100 mM) containing dtpa (100 μM). The absorption spectra were recorded immediately after bolus addition of ONOO$^-$ (resulting in the 0–200 μM peroxynitrite concentration in the sample). The concentration of the ABTS radical cation was calculated based on the measured absorbance at 420 nm (ABTS radical cation molar absorption coefficient $\varepsilon_{420\ nm}$ = 3.6 × 10^4 M^{-1}cm^{-1}). Each point represents the average value of three samples. The error bars represent standard deviations.

much stronger inhibitory effects of ascorbate on the yield of *o*-MitoPhOH and *o*-MitoPhNO$_2$ than those observed. One can assume that all of these reductants are also able to react with the nitrogen dioxide radical ($^{\bullet}$NO$_2$) and/or phenyl radicals. As shown in Figure 5, all of the reductants had little or no effect on the product yield ratios of *o*-MitoPhOH and *o*-MitoPhNO$_2$ formed from the *o*-MitoPhB(OH)$_2$ reaction with peroxynitrite.

To fully understand the mechanistic basis for the differences in product formation from the reaction between ONOO$^-$ and MitoPhB(OH)$_2$ isomers, we quantitated the amount of oxidizing radicals using ABTS, a potent radical scavenger. ABTS can be oxidized to its stable radical cation, ABTS$^{\bullet+}$, by radical species generated in the boronic acid/peroxynitrite system: phenylperoxyl, phenoxyl, and $^{\bullet}$NO$_2$ radicals.[31−36] Formation of the ABTS radical cation can be monitored by EPR or spectrophotometry (at 420 nm, ε = 3.6 × 10^4 M^{-1}cm^{-1}, and at 735 nm, ε = 1.6 × 10^4 M^{-1}cm^{-1}). As shown in Figure 6A and B, the oxidation of ABTS by ONOO$^-$-derived radicals was decreased in the presence of *para* and *meta* isomers of MitoPhB(OH)$_2$ and was almost completely suppressed by *o*-MitoPhB(OH)$_2$. Of note, in the absence of boronates, the yield of ABTS radical cation decreased with increasing concentration of peroxynitrite (Figure 6B). This can be explained by the reaction between ONOO$^-$ and ONOOH (k ~3 × 10^4 M^{-1}s^{-1}).[37]

Elucidation of Radical Pathway: Spin-Trapping of Phenyl Radical Intermediates. The EPR study using MNP spin-trap was performed primarily to detect and characterize radical intermediates formed during the reaction between peroxynitrite and isomers of MitoPhB(OH)$_2$. Previously, we have shown that the phenyl radicals generated during the ONOO$^-$/arylboronate reaction can be trapped with MNP or DEPMPO spin-traps. The EPR spectrum of the MNP-phenyl adduct is more informative (i.e., reveals hyperfine couplings from the aromatic ring protons) than the EPR spectrum of the DEPMPO-phenyl adduct. The addition of a bolus amount of peroxynitrite to incubations containing *p*-MitoPhB(OH)$_2$ or *m*-

dx.doi.org/10.1021/tx300499c | Chem. Res. Toxicol. XXXX, XXX, XXX−XXX

MitoPhB$(OH)_2$, and MNP (pH 7.4) resulted in a multiline spectrum that can be assigned to the corresponding MNP-phenyl radical adduct based on the hyperfine coupling values (Figure 7; Table 1).[12] The multiline EPR spectrum of the

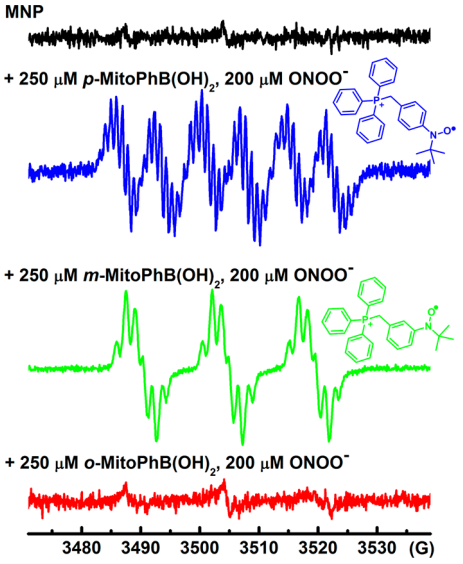

Figure 7. Spin-trapping of phenyl radicals formed from the reaction between $ONOO^-$ and MitoPhB$(OH)_2$. Incubation mixtures contained the following compounds: MitoPhB$(OH)_2$ (250 μM), MNP (40 mM) in phosphate buffer (100 mM, pH 7.4) containing dtpa (100 μM), and 5% CH_3CN. The reaction mixture was transferred to an EPR capillary immediately after bolus addition of $ONOO^-$ (resulting in the 200 μM peroxynitrite concentration in the sample), and the spectra were recorded at room temperature.

Table 1. Hyperfine Coupling Constants of MNP Spin Adducts

	hyperfine splitting constants [G]
m-MitoPhB$(OH)_2$	a(N) = 14.58; a(1H) = 1.82; a(1H) = 1.48; a(1H) = 1.38
p-MitoPhB$(OH)_2$	a(N) = 14.43; a_{ortho}(2H) = 1.86; a_{meta}(2H) = 0.90; a(P) = 6.46

adduct of *p*-MitoPh radical to MNP trap shows an additional hyperfine coupling (a_P = 6.46 G) due to the presence of a phosphorus atom (I = 1/2) in the TPP cation and a significant spin density at the para position (Figure 7). Incubation of peroxynitrite with *o*-MitoPhB$(OH)_2$ did not result in the formation of a similar multiline EPR spectrum. This further suggests a rapid radical−radical recombination mechanism between *o*-MitoPh$^\bullet$ radicals and $^\bullet NO_2$ inside the solvent cage.

Arylboronate Isomers as Potential Antinitration Antioxidants. Previously, we showed that boronates are efficient scavengers of $ONOO^-$ and other oxidants.[11,13,38] Nitration of tyrosyl residues in proteins perturb their functional activity.[39−43] Thus, the ability to prevent $ONOO^-$-mediated tyrosyl nitration is very significant. The finding that *o*-MitoPhB$(OH)_2$ almost completely blocked $ONOO^-$-dependent oxidation of ABTS implies that this class of compounds could be used as potent antioxidants/antinitration agents. To this end, we investigated the effect of isomers of MitoPhB$(OH)_2$ on $ONOO^-$-induced nitration and oxidation of tyrosine. Tyrosine nitration was monitored spectroscopically at 440 nm, while HPLC was used to follow both nitration and oxidation of tyrosine induced by $ONOO^-$. Incubation mixtures contained 2.5 mM tyrosine and 500 μM MitoPhB$(OH)_2$ in phosphate buffer (pH 7.4, 100 mM) containing dtpa (100 μM). The reaction was initiated with the rapid addition of $ONOO^-$. The absorption spectra were recorded after a bolus addition of $ONOO^-$ (final concentration in the 0−400 μM range), and the absorbance at 440 nm was plotted as a function of $ONOO^-$ concentration (Figure 8A). The HPLC analyses were performed using the same conditions. Both nitrotyrosine and dityrosine were quantified by HPLC analyses of the reaction mixtures (Figure 8B). Figure 8A and B shows the inhibitory effect of isomers of MitoPhB$(OH)_2$ on tyrosine nitration and oxidation. Nitrotyrosine formation was attenuated by 87 ± 6%, 59 ± 5%, and 56 ± 5% in the presence of *o*-MitoPhB$(OH)_2$, *m*-

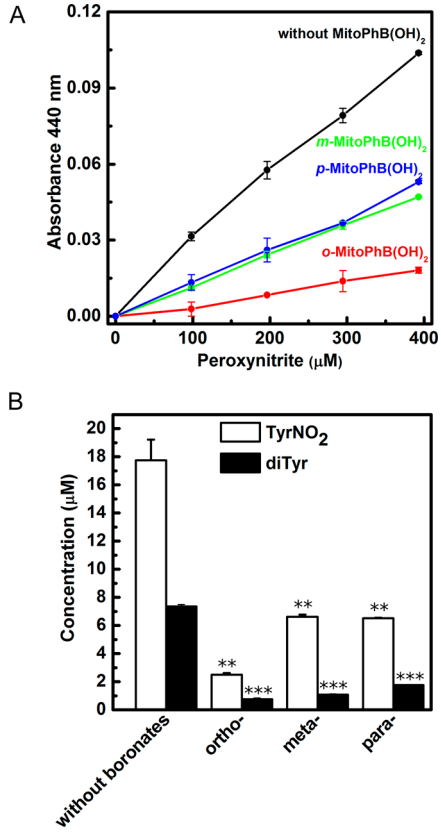

Figure 8. Inhibition of peroxynitrite-induced tyrosine nitration and oxidation by MitoPhB$(OH)_2$. (A) Formation of nitrotyrosine was monitored spectroscopically at 440 nm. Incubation mixtures consisted of 2.5 mM tyrosine and 500 μM MitoPhB$(OH)_2$ (as indicated) in phosphate buffer (pH 7.4, 100 mM) containing dtpa (100 μM). The absorption spectra were recorded after bolus addition of $ONOO^-$ (resulting in the 0−400 μM peroxynitrite concentration in the sample). Each point represents the average value of three samples. The error bars represent standard deviations. (B) Formation of nitrotyrosine and dityrosine was monitored by HPLC. Incubation mixtures consisted of 2.5 mM tyrosine and 500 μM MitoPhB$(OH)_2$ (as indicated) in phosphate buffer (pH 7.4, 100 mM) containing dtpa (100 μM). The HPLC analyses were performed after bolus addition of $ONOO^-$ (resulting in the 400 μM peroxynitrite concentration in the sample). Each bar represents the average value of three samples. The error bars represent standard deviations. Student's unpaired *t* test was used to determine the statistical significance of differences between the formation of nitrotyrosine (or dityrosine) in the absence and presence of the appropiate MitoPhB$(OH)_2$ isomer. *P* values of <0.01 and <0.001 were considered as significant and highly significant, respectively (marked with ** and ***, respectively).

dx.doi.org/10.1021/tx300499c | Chem. Res. Toxicol. XXXX, XXX, XXX−XXX

MitoPhB(OH)$_2$, and *p*-MitoPhB(OH)$_2$, respectively. The dityrosine formation was also inhibited by 89%, 85%, and 76% in the presence of *o*-MitoPhB(OH)$_2$, *m*-MitoPhB(OH)$_2$, and *p*-MitoPhB(OH)$_2$, respectively.

Theoretical Studies. DFT quantum mechanical calculations were performed to characterize the postulated key intermediates formed on the radical pathway of MitoPhB(OH)$_2$ reaction with peroxynitrite, namely, the MitoPhB(OH)$_2$O$^{\bullet-}$ radical anions. We assumed that the radical anions MitoPhB(OH)$_2$O$^{\bullet-}$ formed upon the homolytic O–O bond cleavage undergo further fragmentation resulting in MitoPh$^{\bullet}$ phenyl radical formation. Starting from the optimized structures of the appropriate MitoPhB(OH)$_2$O$^{\bullet-}$ radical anion, we computed a potential energy curve based on which the respective transition state of the fragmentation process was found. According to the PCM/M06-2X/6-31+G(d,p) calculations, the Gibbs energies of activation for the boron–carbon (B–C) bond cleavage in the MitoPhB(OH)$_2$O$^{\bullet-}$ radical anions are 16.3, 26.4, and 27.2 kcal/mol for the *ortho*-, *meta*-, and *para*-isomers, respectively. Table 2 contains the most important structure parameters of MitoPhB(OH)$_2$O$^{\bullet-}$ radical anions and the transition states of their fragmentation reactions. Analysis of spin densities clearly indicates that the majority of radical character in MitoPhB(OH)$_2$O$^{\bullet-}$ radical anions is located on the O$^{\bullet-}$ oxygen atom, whereas in the transition state, it is partially carried by the carbon atom of the phenyl ring being attached to boron. Complete geometries and calculated energies for MitoPhB(OH)$_2$O$^{\bullet-}$ isomers and corresponding transition states are included in Supporting Information.

Table 2. Structural Parameters of MitoPhB(OH)$_2$O$^{\bullet-}$ Radical Anions and the Transition States (TS) of the Fragmentation Reactions[a]

	MitoPhB(OH)$_2$O$^{\bullet-}$			TS			
	B–C (Å)	O spin density	C spin density	B–C (Å)	O spin density	C spin density	$\Delta E^{\#}$ [kJ/mol]
para-	1.65	0.87	0.12	2.21	0.25	0.80	27.2
meta-	1.65	0.87	0.11	2.19	0.27	0.79	26.4
ortho-	1.67	0.93	0.05	1.99	0.48	0.49	16.3

[a] $\Delta E^{\#}$ represents the Gibbs energy of activation of C–B bond cleavage, according to the DFT calculations performed.

Oxidation of *o*-MitoPhB(OH)$_2$ by *in Situ* Generated ONOO$^-$. The oxidation of *o*-MitoPhB(OH)$_2$ was investigated in the presence of O$_2^{\bullet-}$ and $^{\bullet}$NO generating systems. *o*-MitoPhB(OH)$_2$ (100 μM) was incubated with HX (40 μM) and XO (1 mU/mL) in phosphate buffer (50 mM, pH 7.4) containing dtpa (100 μM) for 1 h at room temperature. Similar incubations were performed in the presence of nitric oxide donor, DPTA-NONOate (250 μM). The products were analyzed by HPLC (Figure 9A). In the absence of DPTA-NONOate, there was a modest conversion of *o*-MitoPhB(OH)$_2$ to *o*-MitoPhOH that was attributed to a slow oxidation of boronate by H_2O_2. In incubation mixtures containing DPTA-NONOate and HX/XO, the rate of *o*-MitoPhB(OH)$_2$ oxidation was significantly enhanced along with the formation of *o*-MitoPhNO$_2$. These results further confirm our notion that ONOO$^-$, whether added as a bolus or generated *in situ*, forms the specific nitrated product *o*-MitoPhNO$_2$ in the presence of the *ortho* isomer.

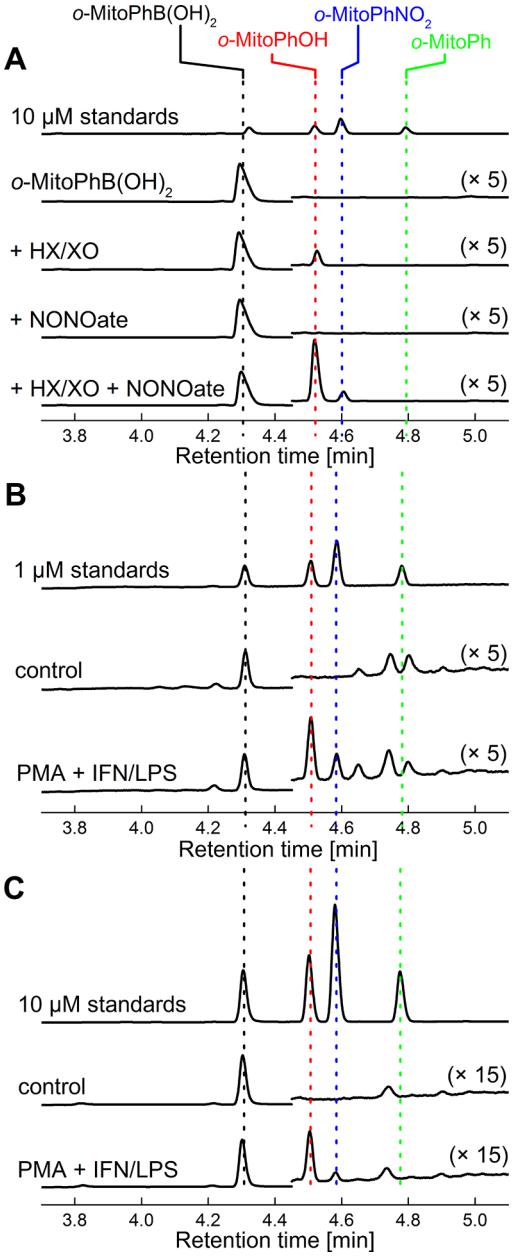

Figure 9. HPLC analyses of products formed from oxidation of *o*-MitoPhB(OH)$_2$ by ONOO$^-$ generated *in situ* in cell-free and cellular systems. (A) Incubation mixtures contained 100 μM *o*-MitoPhB(OH)$_2$, HX (40 μM), and XO (1 mU/mL) in phosphate buffer (pH 7.4, 50 mM) containing 100 μM dtpa, in the presence or absence of DPTA-NONOate (250 μM). After a 1 h incubation at room temperature, the products were analyzed as described in the Experimental Procedures section. (B) RAW 264.7 macrophages were activated using LPS (1 μg/mL), IFNγ (50 U/mL), and PMA (1 μM), and incubated for 1 h with *o*-MitoPhB(OH)$_2$ (50 μM) in DPBS supplemented with glucose and pyruvate as described in the Experimental Procedures section. After incubation, the cells were lysed and the lysate deproteinized before HPLC analysis. (C) The same as in panel B, but cell media were analyzed.

Cell Culture Study. As a proof of concept, we used the macrophage-like RAW 264.7 cells as a model system. Activated RAW 264.7 cells produce ONOO$^-$. We tested whether incubation of *o*-MitoPhB(OH)$_2$ in activated RAW cells would form this nitrated product, *o*-MitoPhNO$_2$ (Figures 9B and C). We measured by HPLC both cell extracts and extracellular

dx.doi.org/10.1021/tx300499c | Chem. Res. Toxicol. XXXX, XXX, XXX–XXX

Scheme 2

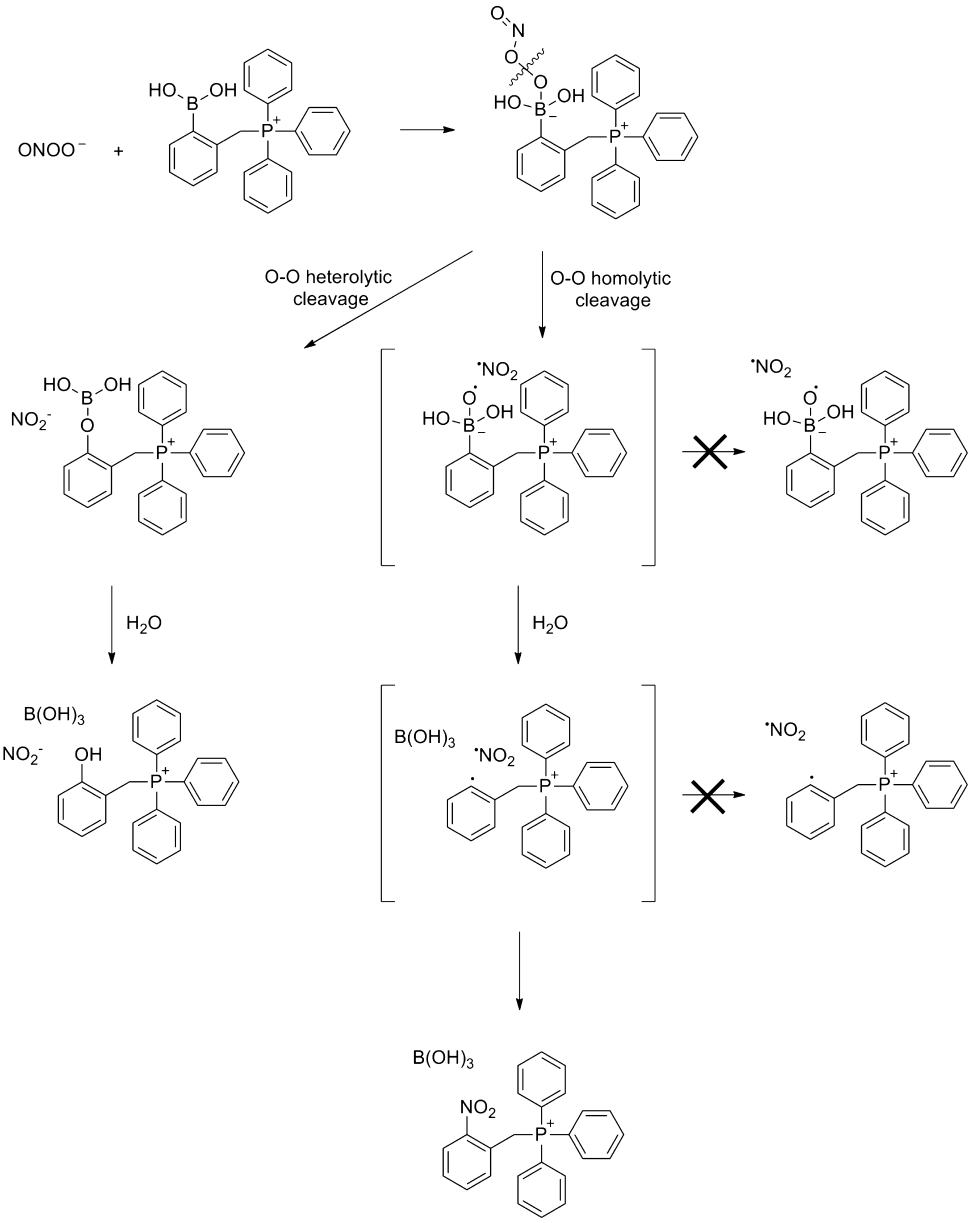

medium. Using boronate-based fluorogenic probes, we have shown previously that macrophages produce $ONOO^-$ after stimulation with lypopolysaccharide (LPS), interferon γ (IFNγ), and phorbol 12-myristate-13-acetate (PMA). As shown in Figure 9B, no oxidation of *o*-MitoPhB$(OH)_2$ is observed in nonstimulated cells. However, when the macrophages are activated to produce peroxynitrite, both *o*-MitoPhOH and *o*-MitoPhNO_2 can be detected. As *o*-Mito PhNO_2 is not formed during the oxidation of *o*-MitoPhB$(OH)_2$ by other oxidants (or by $^{\bullet}NO_2$ formed by MPO), this means that $ONOO^-$ is actually produced in this system.

DISCUSSION

Here, we report the study on the product formation profile for the reactions of isomeric mitochondria-targeted arylboronates with peroxynitrite. HPLC analyses showed that the major products of MitoPhB$(OH)_2$ oxidation by peroxynitrite in the case of all isomers are the corresponding phenols (~90% yield), but the relative yields of the minor product of the reaction between $ONOO^-$ and MitoPhB$(OH)_2$ are different. With *para* and *meta* isomers, the dominant minor product formed from the radical pathway in the presence of 10% 2-PrOH (an effective phenyl radical scavenger) is MitoPh, which is formed by a hydrogen atom abstraction from 2-PrOH by MitoPh$^{\bullet}$ radicals. With the *ortho* isomer, the only minor product detected was *o*-MitoPhNO_2, suggesting a rapid fragmentation of MitoPhB$(OH)_2O^{\bullet-}$ and subsequent recombination of the phenyl radical with $^{\bullet}NO_2$ in the solvent cage. The *ortho* isomer forms a diagnostic marker product in the presence of $ONOO^-$, which strongly suggests that there are significant differences in the decomposition pathway of the boronate–peroxynitrite intermediate in the radical cage. Support for the phenyl radical intermediate came from EPR spin-trapping experiments.

Previously, it was reported that *m*-MitoPhB$(OH)_2$ (MitoB) can be used for the detection and quantitation of mitochondria-

dx.doi.org/10.1021/tx300499c | *Chem. Res. Toxicol.* XXXX, XXX, XXX–XXX

derived hydrogen peroxide.[9,10] In this study, we show that *m*-MitoPhB$(OH)_2$ and other isomers (*o*- and *p*-MitoPhB-$(OH)_2$)[11,13,38] also react with $ONOO^-$. As with simple arylboronates, the peroxynitrite adduct to the boronate moiety decays via two pathways: the heterolysis of the O−O bond (the major pathway) leading to the formation of the corresponding phenols and nitrite and the homolysis of the O−O bond (the minor reaction) that results in the formation of a radical anion, MitoPhB$(OH)_2O^{\bullet-}$, and nitrogen dioxide. According to the DFT quantum mechanical calculations, the energy barrier for the decomposition of the *o*-MitoPhB$(OH)_2O^{\bullet-}$ radical anion, leading to the formation of *o*-MitoPh$^\bullet$ radicals (~16 kJ/mol), is lower than the energy barrier for the fragmentation of *meta* and *para* isomeric MitoPhB$(OH)_2O^{\bullet-}$ radical anions (~27 kJ/mol). This strongly suggests the possibility of rapid and spontaneous *o*-MitoPhB$(OH)_2O^{\bullet-}$ fragmentation, resulting in the formation of *o*-MitoPh$^\bullet$ radical and its subsequent reaction with the $^\bullet NO_2$ radical within the solvent cage. It has to be noted that in case of *meta* and *para* isomers, the radical anion MitoPhB$(OH)_2O^{\bullet-}$ also undergoes spontaneous fragmentation, which is consistent with the low energy barrier. However, in the presence of the phenyl radical scavenger (2-PrOH), the yield of MitoPhNO_2 products is almost 10-fold lower than that for the *ortho* isomer, most probably due to the less efficient radical recombination within the solvent cage. The overall mechanism can be summarized as shown in Scheme 2. The hydrogen atom donors (ABTS, GSH, NADH, and ascorbate) were unable to prevent the formation of *o*-MitoPhNO_2. The EPR spin-trapping experiments with *o*-MitoPhB$(OH)_2$ and $ONOO^-$ did not provide major evidence for trappable radical intermediates, consistent with a rapid recombination of *o*-MitoPh$^\bullet$ and $^\bullet NO_2$ radicals in the solvent cage. In addition, the formation of other oxidizing and nitrating radicals formed from the reaction between $ONOO^-$ and *o*-MitoPhB$(OH)_2$ was minimal, leading to an effective attenuation of $ONOO^-$-mediated tyrosyl nitration. *o*-MitoPhNO_2 formed in relatively high yields ($\eta \approx 9\%$) can be used as a diagnostic biomarker of $ONOO^-$ in cellular and biological systems. In contrast, $ONOO^-$-dependent oxidation of *meta* and *para* isomers of MitoPhB$(OH)_2$ results in the formation of free MitoPh$^\bullet$ radicals that can be scavenged by oxygen and hydrogen atom donors or trapped with MNP and DEPMPO spin traps to give characteristic EPR spectra of the corresponding phenyl radical adducts.

The mechanism of the reaction between boronates and peroxynitrite involving both nonradical and radical pathways appears to be quite general. However, it is not clear how other factors, including steric hindrance and electronic effects of substituents, influence the stability of the key reaction intermediates (e.g., boronate-$ONOO^-$ anionic adduct and R-$B(OH)_2O^{\bullet-}$ radical anion) leading to specific product formation. On the basis of the present results obtained with *o*-MitoPhB$(OH)_2$, we conclude that the *o*-MitoPhNO_2 formed can be used to unequivocally detect $ONOO^-$ formation in cell-free and cellular systems. Boronate probes containing bulky substituents at the *ortho* position may be used in cells to unequivocally confirm $ONOO^-$ formation, via the specific nitration of the boronate probe. Other oxidants (H_2O_2 and HOCl) that can oxidize boronates do not form nitrated products. The nitration of *ortho*-substituted boronates can also be used to distinguish the formation of $ONOO^-$ and $^\bullet NO_2$ formed from MPO/H_2O_2/NO_2^- reaction. *o*-MitoPhB$(OH)_2$ or similar sterically hindered boronates may be used as a potent antinitration agent for inhibiting tyrosyl nitration of cellular/mitochondrial proteins.

In this study, we report that substitution with a charged, bulky group at the *ortho* position (not *meta* or *para* position) of phenylboronates dramatically alters product formation (nitrobenzene derivative) in the presence of $ONOO^-$ via the minor radical pathway. All of the isomers yielded nearly the same amount of the major product, the corresponding phenol. These differences in reaction pathways are attributed to the steric hindrance of the bulky group on radical reactions in the solvent cage of the boronate−peroxynitrite intermediate. Results from the EPR spin-trapping experiments showed that MitoPh$^\bullet$ radicals formed from the reaction between $ONOO^-$ and *meta* and *para* isomers (*m*-MitoPhB$(OH)_2$ and *p*-MitoPhB$(OH)_2$) and not from the *ortho* isomer (*o*-MitoPhB$(OH)_2$) could be detected with 2-methyl-2-nitrosopropane (MNP) spin trap. Regardless of the presence of any biological reductants, the $ONOO^-$/*o*-MitoPhB$(OH)_2$ reaction yields the same amount of *o*-MitoPhNO_2. DFT quantum mechanical calculations suggest that the energy barrier for the dissociation of the *o*-MitoPhB$(OH)_2O^{\bullet-}$ radical anion is lower than that for *m*-MitoPhB$(OH)_2O^{\bullet-}$ and *p*-MitoPhB$(OH)_2O^{\bullet-}$ radical anions, which explains the fast recombination of radicals formed within the solvent cage. Future studies will focus on the applicability of the *ortho* isomer probe described here or its long-chain analogue for the detection of mitochondrial $ONOO^-$ generation.

■ ASSOCIATED CONTENT

Ⓢ Supporting Information

Optimized geometries of all stationary points; mass spectrometry data identifying the products of peroxynitrite oxidation of *o*-, *m*-, and *p*-MitoPhB$(OH)_2$, as well as the products formed from *o*-MitoPhB$(OH)_2$ in MPO/H_2O_2/nitrite system. This material is available free of charge via the Internet at http://pubs.acs.org.

■ AUTHOR INFORMATION

Corresponding Authors

*Institute of Applied Radiation Chemistry, Lodz University of Technology, Zeromskiego 116, 90-924 Lodz, Poland. Tel: +48 42 631 31 70. E-mail: adam.sikora@p.lodz.pl.

*Department of Biophysics, Medical College of Wisconsin, 8701 Watertown Plank Road, Milwaukee, WI 53226. Tel: 414-955-4000. Fax: 414-955-6512. E-mail: balarama@mcw.edu.

Funding

This work was performed with the help of a grant (R01 HL063119) funded by the National Institutes of Health awarded to B.K. A.S. was supported the grant from the Foundation for Polish Science (FNP) within the "Homing Plus" program, and the grant coordinated by JCET, No. POIG.01.01.02-00-069/09 (both grants are supported by the European Union from the resources of the European Regional Development Fund under the Innovative Economy Programme).

Notes

The authors declare no competing financial interest.

■ ACKNOWLEDGMENTS

Access to supercomputing facilities at Cyfronet (Poland) is gratefully acknowledged. We thank Mrs. Monika Zielonka for her assistance with cell culture experiments.

ABBREVIATIONS

2-PrOH, 2-propanol; ABTS, 2,2′-azino-bis(3-ethylbenzothiazoline-6-sulfonate); dtpa, diethylenetriaminepentaacetic acid; DFT, Density Functional Theory; diTyr, dityrosine; DMEM, Dulbecco's modified Eagle's medium; DPBS, Dulbecco's phosphate-buffered saline; FBS, fetal bovine serum; HX, hypoxanthine; IFNγ, interferon γ; LPS, lypopolysaccharide; *m*-MitoPhB(OH)$_2$, (3-boronobenzyl)triphenylphosphonium cation; MitoPh, benzyltriphenylphosphonium cation; *m*-MitoPhOH, (3-hydroxybenzyl)triphenylphosphonium cation; *m*-MitoPhNO$_2$, (3-nitrobenzyl)triphenylphosphonium cation; MNP, 2-methyl-2-nitrosopropane; MPO, myeloperoxidase; $^{\bullet}$NO, nitric oxide (IUPAC-recommended names for nitric oxide are nitrogen monoxide or oxidonitrogen(•)); $^{\bullet}$NO$_2$, nitrogen dioxide; *o*-MitoPhB(OH)$_2$, (2-boronobenzyl)-triphenylphosphonium cation; *o*-MitoPhOH, (2-hydroxybenzyl)triphenylphosphonium cation; *o*-MitoPhNO$_2$, (2-nitrobenzyl)triphenylphosphonium cation; $O_2^{\bullet-}$, superoxide radical anion; ONOO$^-$/ONOOH, peroxynitrite (IUPAC-recommended names for peroxynitrite anion and peroxynitrous acid are oxidoperoxidonitrate(1−) and (dioxidanido)-oxidonitrogen, respectively); PMA, phorbol 12-myristate-13-acetate; *p*-MitoPhB(OH)$_2$, (4-boronobenzyl)-triphenylphosphonium cation; *p*-MitoPhOH, (4-hydroxybenzyl)triphenylphosphonium cation; *p*-MitoPhNO$_2$, (4-nitrobenzyl)triphenylphosphonium cation; DPTA-NONOate, ((*Z*)-1-[*N*-(3-aminopropyl)-*N*-(3-ammoniopropyl)-amino]diazen-1-ium-1,2-diolate); Ph$^{\bullet}$, phenyl radical; SOD, superoxide dismutase; TFA, trifluoroacetic acid; TyrNO$_2$, nitrotyrosine; X, xanthine; XO, xanthine oxidase

REFERENCES

(1) Dikalov, S. I., and Harrison, D. G. (2012) Methods for detection of mitochondrial and cellular ROS. *Antioxid. Redox Signaling*, DOI: 10.1089/ars.2012.4886.

(2) Smith, R. A., Hartley, R. C., and Murphy, M. P. (2011) Mitochondria-targeted small molecule therapeutics and probes. *Antioxid. Redox Signaling 15*, 3021−3038.

(3) Murphy, M. P. (2008) Targeting lipophilic cations to mitochondria. *Biochim. Biophys. Acta 1777*, 1028−1031.

(4) Ainley, A. D., and Challenger, F. (1930) Studies of the boron-carbon linkage. Part I. The oxidation and nitration of phenyl-boric acid. *J. Chem. Soc.*, 2171−2180.

(5) Lo, L. C., and Chu, C. Y. (2003) Development of highly selective and sensitive probes for hydrogen peroxide. *Chem. Commun.*, 2728−2729.

(6) Chang, M. C., Pralle, A., Isacoff, E. Y., and Chang, C. J. (2004) A selective, cell-permeable optical probe for hydrogen peroxide in living cells. *J. Am. Chem. Soc. 126*, 15392−15393.

(7) Dikalov, S. I., Kirilyuk, I. A., Voinov, M., and Grigor'ev, I. A. (2011) EPR detection of cellular and mitochondrial superoxide using cyclic hydroxylamines. *Free Radical Res. 45*, 417−430.

(8) Dickinson, B. C., and Chang, C. J. (2008) A targetable fluorescent probe for imaging hydrogen peroxide in the mitochondria of living cells. *J. Am. Chem. Soc. 130*, 9638−9639.

(9) Cocheme, H. M., Quin, C., McQuaker, S. J., Cabreiro, F., Logan, A., Prime, T. A., Abakumova, I., Patel, J. V., Fearnley, I. M., James, A. M., Porteous, C. M., Smith, R. A., Saeed, S., Carre, J. E., Singer, M., Gems, D., Hartley, R. C., Partridge, L., and Murphy, M. P. (2011) Measurement of H_2O_2 within living Drosophila during aging using a ratiometric mass spectrometry probe targeted to the mitochondrial matrix. *Cell Metab. 13*, 340−350.

(10) Cocheme, H. M., Logan, A., Prime, T. A., Abakumova, I., Quin, C., McQuaker, S. J., Patel, J. V., Fearnley, I. M., James, A. M., Porteous, C. M., Smith, R. A., Hartley, R. C., Partridge, L., and Murphy, M. P. (2012) Using the mitochondria-targeted ratiometric mass spectrometry probe MitoB to measure H2O2 in living Drosophila. *Nat. Protoc. 7*, 946−958.

(11) Sikora, A., Zielonka, J., Lopez, M., Joseph, J., and Kalyanaraman, B. (2009) Direct oxidation of boronates by peroxynitrite: mechanism and implications in fluorescence imaging of peroxynitrite. *Free Radical Biol. Med. 47*, 1401−1407.

(12) Sikora, A., Zielonka, J., Lopez, M., Dybala-Defratyka, A., Joseph, J., Marcinek, A., and Kalyanaraman, B. (2011) Reaction between peroxynitrite and boronates: EPR spin-trapping, HPLC Analyses, and quantum mechanical study of the free radical pathway. *Chem. Res. Toxicol. 24*, 687−697.

(13) Zielonka, J., Sikora, A., Joseph, J., and Kalyanaraman, B. (2010) Peroxynitrite is the major species formed from different flux ratios of co-generated nitric oxide and superoxide: direct reaction with boronate-based fluorescent probe. *J. Biol. Chem. 285*, 14210−14216.

(14) Zielonka, J., Zielonka, M., Sikora, A., Adamus, J., Joseph, J., Hardy, M., Ouari, O., Dranka, B. P., and Kalyanaraman, B. (2012) Global profiling of reactive oxygen and nitrogen species in biological systems: high-throughput real-time analyses. *J. Biol. Chem. 287*, 2984−2995.

(15) Beckman, J. S., Beckman, T. W., Chen, J., Marshall, P. A., and Freeman, B. A. (1990) Apparent hydroxyl radical production by peroxynitrite: implications for endothelial injury from nitric oxide and superoxide. *Proc. Natl. Acad. Sci. U.S.A. 87*, 1620−1624.

(16) Ferrer-Sueta, G., and Radi, R. (2009) Chemical biology of peroxynitrite: kinetics, diffusion, and radicals. *ACS Chem. Biol. 4*, 161−177.

(17) Morrison, D. E., Issa, F., Bhadbhade, M., Groebler, L., Witting, P. K., Kassiou, M., Rutledge, P. J., and Rendina, L. M. (2010) Boronated phosphonium salts containing arylboronic acid, closo-carborane, or nido-carborane: synthesis, X-ray diffraction, in vitro cytotoxicity, and cellular uptake. *J. Biol. Inorg. Chem. 15*, 1305−1318.

(18) Bohle, D. S., Glassbrenner, P. A., and Hansert, B. (1996) Syntheses of pure tetramethylammonium peroxynitrite. *Methods Enzymol. 269*, 302−311.

(19) Hrabie, J. A., Klose, J. R., Wink, D. A., and Keefer, L. K. (1993) New nitric oxide-releasing zwitterions derived from polyamines. *J. Org. Chem. 58*, 1472−1476.

(20) Hrabie, J. A., and Keefer, L. K. (2002) Chemistry of the nitric oxide-releasing diazeniumdiolate ("nitrosohydroxylamine") functional group and its oxygen-substituted derivatives. *Chem. Rev. 102*, 1135−1154.

(21) Van Gelder, B., and Slater, E. C. (1962) The extinction coefficient of cytochrome c. *Biochim. Biophys. Acta 58*, 593−595.

(22) Frisch, M. J. et al. (2009) *Gaussian 09*, revision A.02, Gaussian, Inc., Wallingford, CT.

(23) Zhao, Y., Schultz, N. E., and Truhlar, D. G. (2006) Design of density functionals by combining the method of constraint satisfaction with parametrization for thermochemistry, thermochemical kinetics, and noncovalent interactions. *J. Chem. Theory Comput. 2*, 364−382.

(24) Zhao, Y., and Truhlar, D. G. (2008) Density functionals with broad applicability in chemistry. *Acc. Chem. Res. 41*, 157−167.

(25) Hariharan, P. C., and Pople, J. A. (1973) The influence of polarization functions on molecular orbital hydrogenation energies. *Theor. Chim. Acta 28*, 213−222.

(26) Francl, M. M., Pietro, W. J., Hehre, W. J., Binkley, J. S., Gordon, M. S., DeFrees, D. J., and Pople, J. A. (1982) Self-consistent molecular orbital methods. XXIII. A polarization-type basis set for second-row elements. *J. Chem. Phys. 77*, 3654−3665.

(27) Miertus, S., Scrocco, E., and Tomasi, J. (1981) Electrostatic interaction of a solute with a continuum. A direct utilization of ab initio molecular potentials for the prevision of solvent effects. *Chem. Phys. 55*, 117−129.

(28) Pople, J. A., and Nesbet, R. K. (1954) Self-consistent orbitals for radicals. *J. Chem. Phys. 22*, 571−572.

(29) Koppenol, W. H., Moreno, J. J., Pryor, W. A., Ischiropoulos, H., and Beckman, J. S. (1992) Peroxynitrite, a cloaked oxidant formed by nitric oxide and superoxide. *Chem. Res. Toxicol. 5*, 834−842.

(30) Kurz, C. R., Kissner, R., Nauser, T., Perrin, D., and Koppenol, W. H. (2003) Rapid scavenging of peroxynitrous acid by monohydroascorbate. *Free Radical Biol. Med. 35*, 1529−1537.
(31) Alfassi, Z. B., Marguet, S., and Neta, P. (1994) Formation and reactivity of phenylperoxyl radicals in aqueous solutions. *J. Phys. Chem. 98*, 8019−8023.
(32) Khaikin, G. I., Alfassi, Z. B., and Neta, P. (1995) Inter- and intramolecular redox reactions of substituted phenylperoxyl radicals in aqueous solutions. *J. Phys. Chem. 99*, 16722−16726.
(33) Alfassi, Z. B., Khaikin, G. I., and Neta, P. (1995) Arylperoxyl radicals. Formation, absorption spectra, and reactivity in aqueous alcohol solutions. *J. Phys. Chem. 99*, 265−268.
(34) Khaikin, G. I., Alfassi, Z. B., and Neta, P. (1995) Formation and reactions of halogenated phenylperoxyl radicals in aqueous alcohol solutions. *J. Phys. Chem. 99*, 11447−11451.
(35) Neta, P., and Grodkowski, J. (2005) Rate constants for reactions of phenoxyl radicals in solution. *J. Phys. Chem. Ref. Data 34*, 109−200.
(36) Forni, L. G., Mora-Arellano, V. O., Packer, J. E., and Willson, R. L. (1986) Nitrogen dioxide and related free radicals: electron-transfer reactions with organic compounds in solutions containing nitrite or nitrate. *J. Chem. Soc., Perkin Trans. 2*, 1−6.
(37) Gupta, D., Harish, B., Kissner, R., and Koppenol, W. H. (2009) Peroxynitrate is formed rapidly during decomposition of peroxynitrite at neutral pH. *Dalton Trans.*, 5730−5736.
(38) Zielonka, J., Sikora, A., Hardy, M., Joseph, J., Dranka, B. P., and Kalyanaraman, B. (2012) Boronate probes as diagnostic tools for real time monitoring of peroxynitrite and hydroperoxides. *Chem. Res. Toxicol. 25*, 1793−1799.
(39) Surmeli, N. B., Litterman, N. K., Miller, A. F., and Groves, J. T. (2010) Peroxynitrite mediates active site tyrosine nitration in manganese superoxide dismutase. evidence of a role for the carbonate radical anion. *J. Am. Chem. Soc. 132*, 17174−17185.
(40) Blanchard-Fillion, B., Souza, J. M., Friel, T., Jiang, G. C., Vrana, K., Sharov, V., Barron, L., Schöneich, C., Quijano, C., Alvarez, B., Radi, R., Przedborski, S., Fernando, G. S., Horwitz, J., and Ischiropoulos, H. (2001) Nitration and inactivation of tyrosine hydroxylase by peroxynitrite. *J. Biol. Chem. 276*, 46017−46023.
(41) Castro, L., Demicheli, V., Tortora, V., and Radi, R. (2011) Mitochondrial protein tyrosine nitration. *Free Radical Res. 45*, 37−52.
(42) Abriata, L. A., Cassina, A., Tortora, V., Marin, M., Souza, J. M., Castro, L., Vila, A. J., and Radi, R. (2009) Nitration of solvent-exposed tyrosine 74 on cytochrome c triggers heme iron-methionine 80 bond disruption. Nuclear magnetic resonance and optical spectroscopy studies. *J. Biol. Chem. 284*, 17−26.
(43) Souza, J. M., Peluffo, G., and Radi, R. (2008) Protein tyrosine nitration–functional alteration or just a biomarker? *Free Radical Biol. Med. 45*, 357−366.